Journal of Thermal Engineering
Web page info: https://jten.yildiz.edu.tr
DOI: 10.18186/thermal.990872

Research Article

Effect of orientation of elliptic tube on the total melting time of latent thermal energy storage systems

Mebrouk BENBRIKA[1], Mohamed TEGGAR[1,*], Mohamed BENBELHOUT[1], Kamal A. R. ISMAIL[2], Said BOUABDALLAH[1]

[1]Laboratory of Mechanics, University of Laghouat, Algeria
[2]School of Mechanical Engineering, University of Campinas, Campinas, SP, Brazil

ARTICLE INFO

Article history
Received: 20 December 2019
Accepted: 08 March 2020

Key words:
Elliptic enclosure; Melting; n-Eicosane; PCM; Thermal storage

ABSTRACT

Encapsulation of Phase Change Materials (PCM) for energy storage, thermal comfort and many other energy applications is receiving much attention due to the fact that material, physical characteristics and geometry of the container can affect drastically the thermal performance of the PCM. Phase change materials have usually low thermal conductivity which impairs their thermal charging and discharging characteristics. Different geometries were investigated including rectangular, cylindrical and spherical with and without extended surfaces to investigate the heat charge processes. Cylindrical geometries of circular sections were intensively investigated while cylinders and tubes with elliptic and elongated cross section received less attention, although they may have better thermal performance for thermal storage. The present numerical investigation is aimed at contributing to better understand the effects of the elliptic geometry and how the different geometrical and operational parameters can affect the thermal performance of the enclosed PCM. The present investigation reports the results of a numerical study on elliptic cylinders containing PCM under melting conditions. The 2D inward melting problem is modeled by using a CFD code. The numerical model is based upon the enthalpy-porosity method along with the finite control volume techniques. The numerical predictions are validated against available experimental results. The inward melting process is analyzed for two orientations of the elliptic enclosures. Due to the flow field effect namely the Rayleigh-Bénard convection, the numerical results showed that the horizontal elliptic enclosure have higher melting rate and hence lower total melting time compared to those of the vertical elliptic enclosure.

Cite this article as: Benbrika M, Teggar M, Benbelhout M, Ismail KAR, Bouabdallah S. Effect of orientation of elliptic tube on the total melting time of latent thermal energy storage systems. J Ther Eng 2021;7(6):1479–1488.

***Corresponding author.**
*E-mail address: m.teggar@lagh-univ.dz

This paper was recommended for publication in revised form by Regional Editor Siamak Hoseinzadeh

Published by Yıldız Technical University Press, İstanbul, Turkey

INTRODUCTION

The ever increasing world population and energy demands to accommodate the growing industries for a wide range of diversified commodities, equipment and products led to increasing negative impacts on the environment. This fact forced the world to try to control these effects and thus reduce their impacts by searching for other energy alternatives. Among the most feasible alternatives for shifting aside fossil fuels are solar and wind energy. The two energy resources are of dominated technology, relatively cheap to manufacture and of relatively high efficiency. Solar energy is widely accepted but its main drawback is that it is intermittent. To remedy this problem energy storage is the key solution independent of the form of energy; if it is electrical batteries are well developed to cope with these necessities. In the case of thermal energy, concepts of latent, sensible and hybrid storage systems are well understood and are widely applied in many relatively big projects. Latent heat storage is technically more attractive than sensible heat storage due to its high thermal capacity and also due its nearly isothermal behavior in comparison with sensible heat storage. Latent heat storage systems incorporate Phase Change Materials (PCMs) because of their high thermal storage density at nearly constant temperature.

Melting of confined phase change materials is of particular importance for several thermal applications such as thermal storage, building energy management and cooling of electronic devices. Earlier numerical investigations on inward solid-liquid phase change were based on heat conduction and neglected however heat convection during phase change process [1–5]. The models are however valid for limited cases of lower values of Rayleigh number. In case of melting, natural heat convection is a key feature of the phase change process.

Melting and solidification in different cavity shapes (rectangular [6–8], sphere [9], tube [10–14] and other geometries [15–17]) were investigated. However, elliptic cross section enclosures received less attention both numerically and experimentally although they could be as efficient as other geometries. In addition, the tubes of elliptic section may be an alternative for circular tubes when there is space restriction. Chen et al. [18] investigated analytically melting of n-octadecane in a horizontal elliptic cylinder. They concluded that the melting rate in the elliptic enclosure is higher than that in the circular cylinder of the same cross sectional area. The melting rate in elongated elliptic enclosures was shown to be higher than that inside oblate enclosures [19].

The melt flow field in a cylinder was examined by Chung et al. [20] for high Rayleigh numbers ($Ra > 10^6$). The rolls of Rayleigh-Bénard convection appeared in the bottom of the cylinder because the melt in the bottom is limited by two solid boundaries (the cold melting front and the hot cylinder wall) which led to thermal instability. For modeling of the melting process, the authors used the enthalpy-porosity method and the finite volume techniques.

Alawadhi [21] investigated the flow patterns in the liquid phase during solidification of water as PCM in an elliptic enclosure for different inclinations (0°, 45° and 90°). The author used the apparent capacity method for modeling of the phase field. The results indicated that there is no significant effect of the enclosure inclination on the solidification rate. Recently, Jourabian et al. [22] reported also that inclination of 90° of the elliptical enclosure does not affect the time for ice melting. The last two investigations [21–22] neglected however the effects of the Rayleigh-Bénard convection which may affect significantly the phase change rate and consequently the melting time.

In the present study, the influence of the flow field on both the melting rate and the time for complete melting is examined in an elliptic enclosure for two inclinations of 0° and 90° in case of melting of n-eicosane. The modeling is based on the enthalpy-porosity method and the finite volume technique. The melting process, the melting rate and particularly the time required for total melting are examined.

PHYSICAL MODEL

The 2D problem of PCM melting in an elliptic enclosure (28 mm, 14 mm) is considered. The schematic of the elliptic enclosure is shown in Fig. 1. The enclosure is supposed to be of negligible thickness. A heat transfer fluid (air) is flowing over the enclosure in which temperature is set to $T_{HTF} > T_f$ and the heat transfer coefficient (h) is supposed constant.

In the subsequent analysis we consider two inclinations with respect to the horizontal line (0° and 90°) i.e. horizontal elongated and vertical elongated enclosures respectively.

The PCM considered is n-eicosane Table 1.

Mathematical Modeling

The 2D PCM internal melting problem in an elliptic container is studied where PCM is initially solid at $T_i < T_f$.

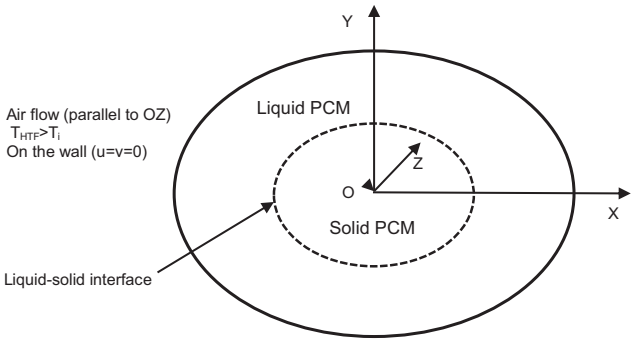

Figure 1. Schematic of the elliptic cavity filled with PCM.

Table 1. Thermophysical properties of n-eicosane [23]

Properties	Values
Melting temperature	308.15–310.15 K
Density	770 kg m^{-1}
Kinematic viscosity	5×10^{-6} m^2 s^{-1}
Specific heat solid/liquid	2.460 KJ kg^{-1} K^{-1}
Thermal conductivity	0.1505 W m^{-1} K^{-1}
Latent heat of fusion	247.6 kJ kg^{-1}
Thermal expansion	0.0009 K^{-1}

The elliptic capsule is fully wetted by the flowing heat transfer fluid (air) at temperature T_{HTF}. The mathematical model describing the melting process is based upon the enthalpy-porosity method [24]. The problems of PCM melting involving natural convection can be divided into two main models: the unconstrained solid model [25–28] and the constrained solid model [29–30]. In the former the solid PCM is supposed to move in the gravity direction whereas in the latter the bulk does not move. However, the constrained model used here is valid for a large class of materials where there are approximately equal solid and liquid phase densities. In the present model, the solid PCM is not absolutely constrained but it can move in the melt because of the buoyancy effect.

The following assumptions are considered in the formulation: (i) the superheat of the PCM is negligible; (ii) the thermal expansion due to phase change is also neglected; (iii) Boussinesq approximation is employed for the buoyancy effect; (iv) the viscous dissipation is neglected.

Under the above conditions the heat transfer in the whole PCM and the melt viscous flow are described by the following conservation equations [31]:

Mass

$$\frac{\partial \rho}{\partial t} + \nabla.(\rho \vec{\vartheta}) = 0 \tag{1}$$

Momentum

$$\frac{\partial}{\partial t}(\rho \vec{\vartheta}) + \nabla.(\rho \vec{\vartheta}\vec{\vartheta}) = -\nabla p + \nabla.(\mu \nabla \vec{\vartheta}) + \rho \vec{g} + \vec{S} \tag{2}$$

Energy

$$\frac{\partial}{\partial t}(\rho H) + \nabla.(\rho \vec{\vartheta} H) = \nabla.(k \nabla T) \tag{3}$$

$\vec{S}$ in Eq.(2) is a source term defined by the Darcy's law to account for melting dynamics in the momentum balance equation. The mushy zone constant is taken 10^6 kg/m^3s. Liquid fractions are defined in the mushy zone as follows.

$$\lambda = \begin{cases} 0 & if \ T \le T_s \\ 1 & if \ T \ge T_l \\ \dfrac{T - T_s}{T_l - T_s} & if \ T_s < T < T_l \end{cases} \tag{4}$$

The PCM is initially solid:

$$\text{At } t = 0: \ T_i < T_f \tag{5}$$

On the enclosure's wall a no slip and a convective heat conditions are considered:

$$u = \vartheta = 0; \frac{\partial T}{\partial x} = h(T_{HTF} - T_w) \tag{6}$$

NUMERICAL PROCEDURE AND GRID OPTIMIZATION

The numerical resolution of the mathematical model was carried out by using a commercial code. Unstructured finite control volumes were employed for meshing. For the discretization of the various model terms, the QUICK scheme was used while the SIMPLE algorithm was employed for the velocity-pressure coupling. For the pressure equation correction, the PRESTO scheme was chosen. Relaxation factors were set 0.3, 0.7, 1 and 0.9 respectively for the pressure, the velocity, the energy and the liquid fraction. Residual convergence values were fixed as: 10^{-3}, 10^{-3} and 10^{-6} respectively for continuity, momentum and energy. However, numerical tests for grid size independence were made. They are presented for the time evolution of the average liquid fraction in the cavity (Fig. 2). The optimum choice for the number of control volumes is 10577. The numerical tests showed that 0.1 s is an optimum choice for the time step (Fig. 3).

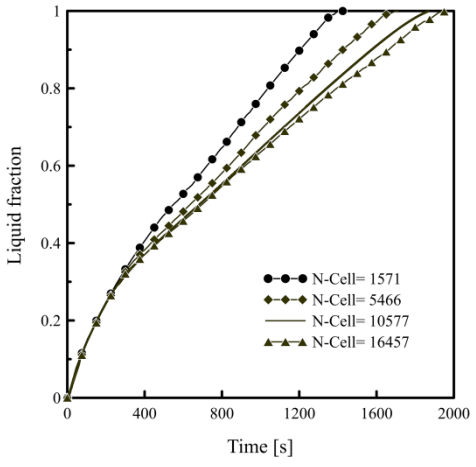

Figure 2. Mesh dependency of the numerical predictions.

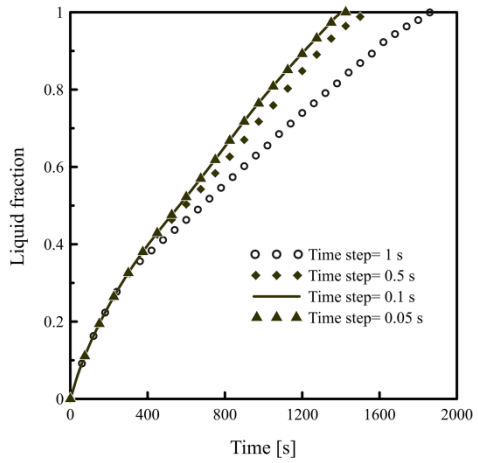

Figure 3. Time step optimization for the present model.

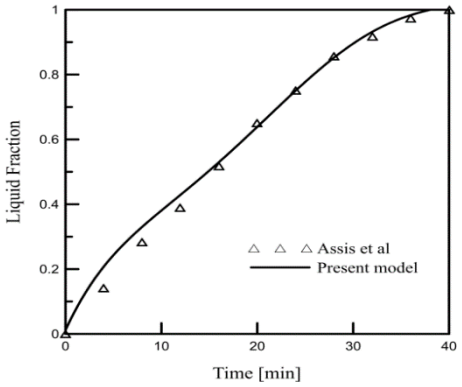

Figure 4. Evolution of liquid fraction versus time: Comparison of the present model with the results of Assis et al. [32].

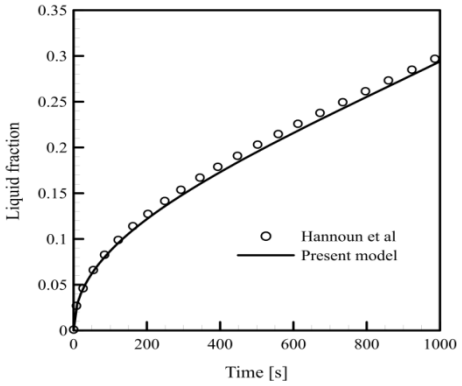

Figure 5. Comparison of the present predictions with the Benchmark results [33].

Validation

The numerical predictions were validated by comparison with experimental results due to Assis et al. [32]. These results are for the melting process of RT27 paraffin wax (Table 2) contained in a spherical glass container of 80 mm inner diameter and 2 mm thickness. The solid PCM was initially kept at its mean melting temperature 29 °C. The container was placed in a water tank at a higher uniform temperature (39 °C). Fig. 4 shows a comparison of the predicted with the experimental results for the liquid fraction evolution. As can be seen, the agreement is good.

Another validation of the numerical predictions was done by comparing with the benchmark results of Hannoun et al. [33] for the melting process of PCM (tin) in a square cavity (0.1 × 0.1 m^2). Tin was initially solid at the melting temperature $T_i = T_f = 505$ K. The cavity was heated from one side wall to a fixed temperature above the melting point (508 K) while the other cold vertical wall was kept at the melting temperature 505 K. The horizontal walls were maintained adiabatic. The thermophysical properties of tin are summarized in Table 3. Fig. 5 shows the predicted variation of the melt fraction with time compared with the benchmark results. As can be seen, good agreement was obtained.

Table 2. Thermophysical properties of RT27 [32]

Properties	Values
Melting temperature	28–30 °C
Density	870 kgm^{-3}
Dynamic viscosity	3.42 10^{-3}kg m^{-1} s^{-1}
Specific heat solid/liquid	2.4/1.8 kJ kg^{-1} K^{-1}
Thermal conductivity solid/liquid	0.24/0.15 $Wm^{-1}K^{-1}$
Latent heat of fusion	179 $kJkg^{-1}$

Table 3. Thermophysical properties of tin [33]

Properties	Values
Melting temperature	505 K
Density	7500 kg m^{-3}
Kinematic viscosity	5x10^{-7} m^2 s^{-1}
Specific heat	200 J kg^{-1} K^{-1}
Thermal conductivity	60 W m^{-1} K^{-1}
Latent heat of fusion	247.6 kJ kg^{-1}
Coefficient of thermal expansion	2.67 10^{-4} K^{-1}

RESULTS AND DISCUSSION

Results are presented for PCM (n-eicosane) melting process in an elliptical enclosure of minor and major axes a = 28 and b = 14 mm, respectively. The melting process in the enclosure is analyzed for two enclosure inclinations of 0° and 90°. The PCM is initially solid at T = 290.15 K. Over the elliptic enclosure, a working fluid (hot air) flows parallel to the tube at constant temperature $T_{HTF} = 325.15$ K.

The convective heat flow between the working fluid and the elliptic capsule wall is considered h = 100 W $m^{-2} K^{-1}$.

Figures 6a–e and 7a–e illustrate for different times (250, 500, 750, 1000 and 1250 s) the temperature distributions, the melt fractions and the streamlines in the elliptic enclosure; two inclinations (0° and 90°) are considered. The left column represents the 0° enclosure inclination while the right column is for the 90° enclosure inclination.

Temperature Distributions

At the early stages of the melting process (250 s), the isotherms are parallel to the capsule's wall for both inclinations (0° and 90°) as can be seen in Fig. 6a. Heat transfer between the hot source and the encapsulated PCM is done mainly by conduction. In the case of 0° enclosure inclination, the maximum temperature is not located at the top; it is located rather on the wall symmetrically towards the major axis while the higher temperatures are in the upper part of the enclosure for the 0° enclosure inclination. At the top of the enclosure, the temperature is 317 K.

At time 500 s, for both cases the melt temperatures are higher in the upper region of the enclosure (Fig. 6-b), the maximum temperature calculated on the top of the horizontal elliptic enclosure is 321 K while in the other case (*i.e.* the vertical enclosure) the maximum temperature is higher than that in the horizontal enclosure (235 K).

In the melt, the isotherms are no longer concentric. In the bottom of the horizontal elongated enclosure, the isotherms are wavy and distorted in the other vertically elongated capsule. Natural heat convection is significant and dominates the heat transfer process.

Figure 6-c indicates that at 750 s the temperatures are higher than 294 K in the whole capsule for both cases. Due to the buoyancy effects, the higher temperatures are always seen to be in the upper part of the enclosure. The highest temperature is located on the top of the enclosure with a value of 325 K; this temperature is nothing but that of the HTF.

The horizontal parallel isotherms in the upper melt region indicate that heat transfer is dominated by conduction at this stage (750 s) in this upper melt region for both enclosure cases (Fig. 6-c). The lower melt temperatures are observed on the horizontal enclosure. The maximum temperature calculated in the top of this enclosure is 321 K; it is lower than that in the case of 90° inclination (325.15 K).

At time 1000 s (Fig. 6-d), one can clearly distinguish between two thermal regions:

- An upper part of thermally stratified melt.
- A lower part with distorted isotherms. Strong distortion results in the apparition of mushrooms shaped isotherms in the bottom of the enclosure of 0° inclination which disappear later (1000 s). Similar findings were also reported by Chunjian et al. [34] on the unconstrained melting of Calcium Chloride hexahydrate in a vertical cylinder.

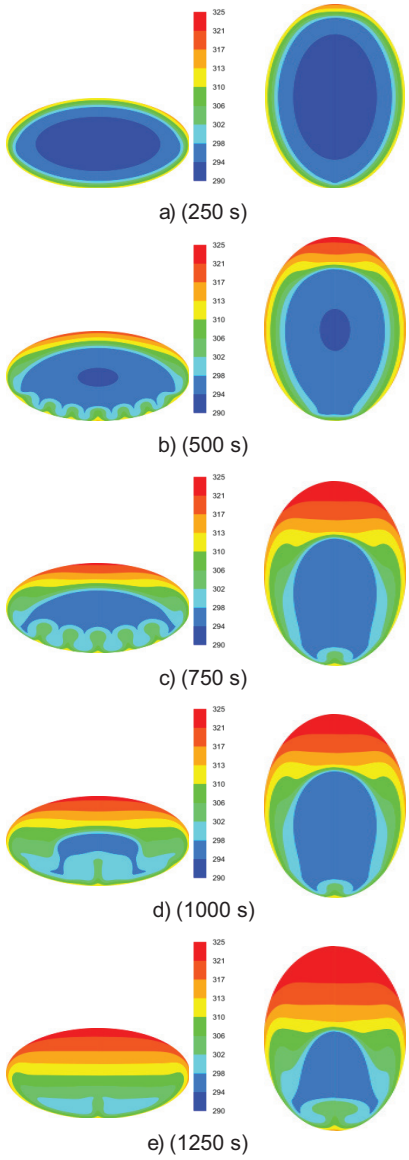

Figure 6. Temperature distribution at different times for two enclosure inclinations 0° and 90°.

The former (upper part) indicates conduction dominant heat transfer while the latter (lower part) indicates convective dominant heat transfer in the melt.

Flow Field

The streamlines are depicted in Figs. 7a-e for two cases i.e horizontal (case 1) and vertical (case 3). The flow patterns are shown at the left hand half of the enclosures. Figure 7a displays the streamlines at 250 s. At this early melting stage, heat flow convection is weak and cannot develop because of the viscous effects of the molten PCM. Therefore, the heat transfer is dominated by the heat conduction mode. This feature at the early stages of melting was confirmed by other investigators in the literature [18, 20, and 22]. However,

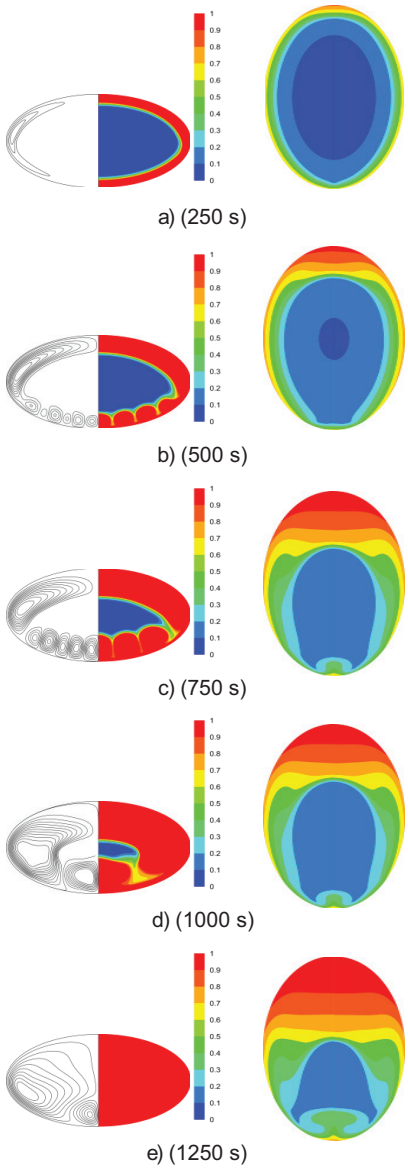

Figure 7. Streamlines and melt fractions for inclinations 0° and 90°.

heat convection can be weak for thin molten layers but also for lower heating levels even though within larger melt layers. These situations are characterized in the literature by low Rayleigh numbers. Therefore, investigators [20, 35, 36] indicated that natural convection is significant only for $Ra > 10^4$ for PCM melting in circular cylinders.

Figure 7b shows the streamlines in the two enclosures at time 500 s. The flow patterns are totally different in these two cases. At this melting stage, two symmetric opposing circulations dominate the melt flow in the whole enclosure of the vertical enclosure. Thus, the melt moves up along the hot capsule wall and goes down along the cold melting front. But, the horizontally elongated capsule showed a quite different flow pattern. The upper part of the melt displays a bi-cellular (counter-rotating) symmetric flow with respect to the vertical axis of the elliptic enclosure; whereas in the bottom a multi-cell flow is observed with weak vortices at this time (500 s). However, the number of these vortices as well as their sizes is mainly defined by the size of the gap; which contains the molten PCM between the lower melting front and the bottom enclosure wall. These vortices are known as Rayleigh-Bénard convection. Apparition of this type of heat convection is due to the fact that the liquid PCM is confined between the hotter enclosure wall and the colder melting front; which can be assimilated to two parallel plates. This type of rolls was also reported in the literature. Chung et al. [20] indicated this kind of rolls in their work on melting in circular cylinders. It is worth mentioning that the present work as well as that of Chung et al. [20] used the same numerical approach (enthalpy-porosity method). These captured rolls are consistent with other works in the literature of pure heat convection (i. e. melting not involved) in concentric circular annulus [23]. The rolls of Rayleigh-Bénard convection contribute significantly to enhancing both heat transfer and melting rate. Thus, the role of these vortices is important in shortening the melting time.

As time advances (750 s), the rolls are strengthened (Fig. 7-c) while in the second enclosure (i.e. 90 ° inclined enclosure) two additional cells appear in the bottom of the enclosure. This flow transition is consistent with results obtained in circular cylinders as indicated in other investigations [37–38].

Later (1000 s), the multiple cells in the bottom of the enclosure (0° inclined) merge and end up with a bi-cellular flow structure (Fig. 7-d). The circulations are slower. Hence, the melting is weaker than the earlier stage. The secondary flow in the 90° inclined enclosure develops to a 4 cells flow (Fig. 7-d) and then to multi-cells flow structure at the late stage of the melting process i.e. 1250 s (Fig. 7-e). Thus, heat convection in the bottom of the enclosure is seen to be more effective. The melting progress is then faster compared with that in the upper region of the enclosure.

In order to show the effect of low heating rate on the Rayleigh-Bénard rolls, a simulation is done with lower heat transfer coefficient ($h = 25\ W.m^{-2}K^{-1}$) at the external surface of the enclosure. Fig. 8 shows the streamlines as well as the variation of the melting fractions at different times. The strength of these rolls is affected by the heating rate. Thus, weaker rolls are obtained with lower heating rate and the number of rolls decreases with time.

Melting Fractions

The melting fractions are shown in the right hand side of the enclosures (Figs. 7a-e). The melt is illustrated by the red color while the solid PCM is in blue color; the other colors show the mushy zone (i. e. between red and blue).

At time 250 s (Fig. 7-a), the symmetric liquid layer is confined between the parallel concentric boundaries consisting

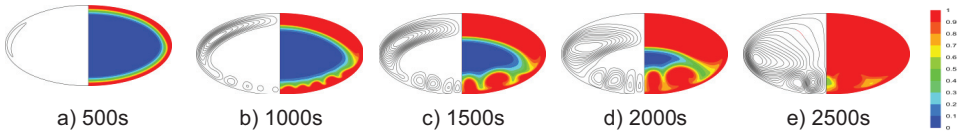

Figure 8. Streamlines and melting fractions under low heating rate (h= 25 W/m K) for the horizontal elliptic enclosure.

of the rigid cavity wall and the solid melting front. Hence, the melting front is advancing uniformly. This means that natural convection is not significant yet. The size of the melt is approximately the same in both enclosure cases.

As time proceeds (500 s), the melt is seen to be large for the two inclination cases (Fig. 7b). The melting front has a wavy shape in the bottom of the enclosure of 0° inclination because of the rolls of Rayleigh-Bénard convection. This wavy shape of the melting front is also reported by Chung et al. [20] where multi cells were captured for the melting problem in a circular cylinder. Later (1000 s), the wavy shape disappears at the late stage of the melting process as shown in Fig 7-d. At this time (i.e. 1000 s), the solid PCM in the 90° inclination case is still important and occupies the lower part of the enclosure. Progress of the melting front is faster in the upper region of the vertical elliptic enclosure.

Time Evolution of The Mean Liquid Fraction

The variations with time of the mean liquid fraction in the two enclosures (horizontal (case 1) and vertical (case 3)) and in circular tube (20 mm Ø) as a reference case (case 2) are depicted in Fig. 9. The mean liquid fraction evolves typically as a function of the time square root. This function depends mainly on the sensible heat and the latent heat exchanged in the PCM, the thermal properties of the material, the geometry, and the heating conditions. This typical behavior can be seen in the curve of the vertically elongated enclosure (case 3). But, in case 1 (horizontal elliptic enclosure), it is clearly seen that the melting rate is enhanced between times 500 s and 750 s. In fact, during this time the multi-cells flow affects strongly the heat transferred and the melting rate. After that, when the multi-rolls merge into two symmetric large cells (Fig. 7d), the melting rate is seen to slow down. Meanwhile, the melting rate in case 3 is monotone. This latter does not, unlike the case 1, show Rayleigh-Bénard convection. It is interesting to note that the entire PCM for horizontal enclosure is melted faster than that in the vertical enclosure, and the latter has approximately similar melting with the circular enclosure (case 2).

Total Melting Time

Figure 10 shows the time for complete melting as function of the heat convection coefficient between the HTF and the enclosure wall for a circular enclosure (20 mmØ) and the elliptic enclosure (vertical and horizontal). One can observe that the increase of the heating rate reduces the

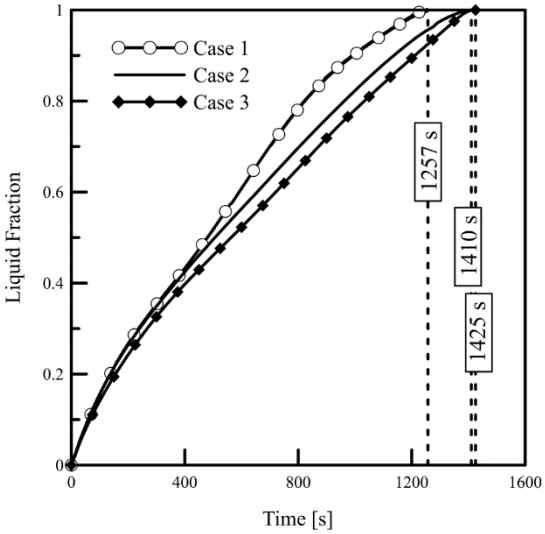

Figure 9. Time evolution of the mean liquid fraction for h = 100 $Wm^{-1}K^{-1}$.

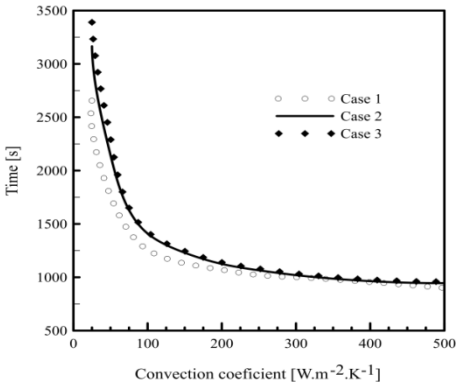

Figure 10. Variation of the time for complete melting with the convection heat coefficient.

time for complete phase change. For higher values of the heat convection coefficient (h > 100 W $m^{-2}K^{-1}$), there no noticeable difference in melting times for the three cases. For h = 100 $Wm^{-2}K^{-1}$, the melting times of n-eicosane in the elliptic enclosure are estimated by 1257 s and 1425 s for the 0° and 90° inclinations respectively. The melting rate is found to be higher in case 1 i.e. the horizontal enclosure. The relative difference is estimated by 10.85%. This difference is mainly due to the effect of the Rayleigh-Bénard

convection in the lower part of the elliptic enclosure (case 1) as shown in Fig. 9.

For h = 50, the total melting times calculated are 1800 s, 2145 s and 2300 s for case 1, case 2 and case 3 respectively. The vertical elliptic enclosure (case 3) takes longer time to melt, then the circular enclosure and finally the horizontal elliptic enclosure shows lower melting time.

For low loading rate (h = 25 $Wm^{-2}K^{-1}$), the total melting times are estimated by 2655 s and 3390 s respectively for the case 1 (0° inclination) and the case 3 (90° inclination). Hence, the relative difference for the low loading rate is estimated by 27.68 % which is found to be higher than that of the high loading rate (10.85 %). The vertical elliptic enclosure (case 3) shows similar heating rate and melting time as those of the circular enclosure (case 2).

However, Jourabian et al. [22] indicated that there is no significant difference between times for total melting inside horizontally and vertically elongated enclosures. In their work the Rayleigh-Bénard convection was not numerically captured in the bottom of the enclosure; which is possibly due to the numerical method used producing indistinguishably close melting times.

CONCLUSIONS

The 2D melting problem of n-eicosane as PCM has been numerically investigated in an elliptic enclosure. The melting process has been examined for two enclosure inclinations (0° and 90°). The numerical results showed the strong effect of the melt flow structure on the melting rate as well as on the complete melting time. In the case of 0° inclination, the Rayleigh-Bénard convection showed melting rate enhancement and hence lower total melting time. For higher values of the heat convection coefficient (h > 100 $Wm^{-2}K^{-1}$), the time for complete melting is not affected by the orientation of the elliptic enclosure. The relative differences between melting times for the two enclosure inclinations (0° and 90°) have been estimated by 10.85% for high loading rate (h = 100 $Wm^{-2}K^{-1}$) and 27.68 % for low loading rate (h = 25 $Wm^{-2}K^{-1}$). Thus, the horizontal enclosure (0° inclination) produces lower total melting time for the charging process if used as a capsule for latent heat storage systems.

NOMENCLATURE

a, b	major and minor axes, m
B	thermal expansion, K^{-1}
c_p	specific heat , J K^{-1} kg^{-1}
μ	dynamic viscosity, pa s
G	gravitational acceleration, m s^{-2}
P	density, kg m^{-3}
H	specific enthalpy, J kg^{-1}
Λ	liquid fraction
H	convection coefficient, W m^{-2} K^{-1}
N	kinematic viscosity, m^2 s^{-1}
K	thermal conductivity, W m^{-1} K^{-1}
L_f	latent heat of fusion, J kg^{-1}
M	masse, kg
S	source term
T	temperature, K
T	time, s
u,v	velocities, m s^{-1}

Subscripts

I	Initial
F	Fusion
L	Liquid
S	Solid
W	Wall

ACKNOWLEDGMENTS

This work is supported by the Algerian Ministry of Higher Education and Scientific Research ((DGRSDT-MESRS) under the framework of a project PRFU (A11N01UN030120190003).

AUTHORSHIP CONTRIBUTIONS

Data, Writing, Analysis: M.B.; Concept, Writing, Literature research, Analysis: M.T.; Data, Writing: M. B.; Writing, Critical revision: K.A.R.I.; Critical revision: S.B.

DATA AVAILABILITY STATEMENT

No new data were created in this study. The published publication includes all graphics collected or developed during the study.

CONFLICT OF INTEREST

The author declared no potential conflicts of interest with respect to the research, authorship, and/or publication of this article.

ETHICS

There are no ethical issues with the publication of this manuscript.

REFERENCES

[1] Ilicali C, Cetin M, Cetin S. Methods for freezing and thawing of ellipses. J Food Eng 1996;28:361–72. [CrossRef]

[2] Voller VR, Cross M. Estimating the solidification/melting times cylindrically symmetric regions. Int J Heat Mass Transf 1981;24:1457–62. [CrossRef]

[3] Fikiin, KA. Generalized numerical modelling of unsteady heat transfer during cooling and

freezing using an improved enthalpy method and quasi-one-dimensional formulation. Int J Ref 1996;19:132–40. [CrossRef]
[4] Pham QT. Shape factors for the freezing time of ellipses and ellipsoids. J Food Eng 1991;13:159–70. [CrossRef]
[5] Teggar M, Mezaache E, Benchatti A, Zeghmati B. Comparative study of heat transfer during solidification of phase change materials inside three different capsules. Int J heat Techn 2010;28:19–23. [CrossRef]
[6] Shokouhmand C, Kamkari B. Experimental investigation on melting heat transfer characteristics of lauric acid in a rectangular thermal storage unit. Exp Therm Fluid Sci 2013;50:201–12. [CrossRef]
[7] Arıcı M, Tütüncü E, Kan M, Karabay H. Melting of nanoparticle-enhanced paraffin wax in a rectangular enclosure with partially active walls. Int J Heat Mass Transf 2017;104:7–17. [CrossRef]
[8] Bondareva NS, Sheremet MA. Numerical simulation of natural convection melting in 2D and 3D enclosures, J Therm Eng 2019;5:51–61. [CrossRef]
[9] Ismail K, Henrıquez J. Numerical and experimental study of spherical capsules packed bed latent heat storage system. App Therm Eng 2002;22:1705–16. [CrossRef]
[10] Ismail KAR, Fátima L, Raquel S, Antonio J, Louryval P. Experimentally validated two dimensional numerical model for the solidification of PCM along a horizontal long tube, Int J Therm Sci 2014;75:184–93. [CrossRef]
[11] Saitoh T, Hirose K. High Rayleigh number solutions to problems of latent heat thermal energy storage in a horizontal cylinder capsule. J Heat Trans 1982;104:545–53. [CrossRef]
[12] Bareiss M, Beer H. An analytical solution of heat transfer process during melting of an unfixed solid phase change material inside a horizontal tube. Int J Heat Mass Transf 1984;27:739–46. [CrossRef]
[13] Prasad A, Sengupta S. Numerical investigation of melting inside a horizontal cylinder including the effect of natural convection. J Heat Transf 1987;109:803–6. [CrossRef]
[14] Nicholas D, Bayazitoglu Y. Heat transfer and melting front within a horizontal cylinder. J Sol Energ Eng 1980;102:229–32. [CrossRef]
[15] Dhaidan N, Khalaf A. Experimental evaluation of the melting behaviours of paraffin within a hemicylindrical storage cell. Int Comm Heat Mass Transf 2020;111;104476. [CrossRef]
[16] Iachachene F, Haddad, Z, Hakan, O, Abu-Nada, E. Melting of phase change materials in a trapezoidal cavity: Orientation and nanoparticles effects. Journal of Molecular Liquids 2019;292:11059. [CrossRef]
[17] Hosseinzadeh K, Mogharrebi A, Asadi A, Paikar M, Ganji D. Effect of fin and hybrid nano-particles on solid process in hexagonal triplex Latent Heat Thermal Energy Storage System. J Molec Liq 2020;300:112347. [CrossRef]
[18] Chen, WZ, Yang, QS, Dai, MQ, Cheng, SM. An analytical solution of the heat transfer process during contact melting of phase change material inside a horizontal elliptical tube. Int J Energ 1998;22:131–40. [CrossRef]
[19] Fomin SA, Wilchinsky A. Shape-factor effect on melting in an elliptic capsule. Int J Heat Mass Transf 2002;45: 3045–54. [CrossRef]
[20] Chung JD, Lee JS, Yoo H. Thermal instability during the melting process in an isothermally heated horizontal cylinder. Int J Heat Mass Transf 1997;40:3899–907. [CrossRef]
[21] Alawadhi E. A solidification process with free convection of water in an elliptical enclosure. Energ Conv and Manag 2009;50:360–4. [CrossRef]
[22] Jourabian, M, Farhadi, M, Darzi, AR. Heat transfer enhancement of PCM melting in 2D horizontal elliptical tube using metallic porous matrix. Theor Comput Fluid Dynam 2016;30:579–603. [CrossRef]
[23] Darzi, AR, Farhadi, M, Sedighi, K. Numerical study of melting inside concentric and eccentric horizontal annulus. App Math Model 2012;36:4080–86. [CrossRef]
[24] Brent, AD, Voller, VR, Reid, KJ. Enthalpy-porosity technique for modeling convection-diffusion phase change: Application to the melting of a pure metal. Num Heat Transf 1988;13:297–318. [CrossRef]
[25] Kozak, Y, Ziskind, G. Novel enthalpy method for modeling of PCM melting accompanied by sinking of the solid phase. Int J Heat Mass Transf 2017;112:568–86. [CrossRef]
[26] Hosseinizadeh, S, Rabienataj, R, Darzi A, Tan, L. Unconstrained melting inside a sphere, Int J Therm Sci 2013;63:55–64. [CrossRef]
[27] Faden, M, König-Haagen, A, Höhlein, S, Brüggemann, D. An implicit algorithm for melting and settling of phase change material inside macrocapsules. Int J Heat Mass Transf 2018;117:757–67. [CrossRef]
[28] Sparrow, EM, Geiger, GT. Melting in a horizontal tube with the solid either constrained or free to fall under gravity. Int J Heat Mass Transf 1986;29:1007–16. [CrossRef]
[29] Hlimi, M, Hamdaoui, S, Mahdaoui, M, Kousksou, T, Ait Msaad, A, Jamil, A, El Bouardi, A. Melting inside a horizontal cylindrical capsule. Case Stud Thermal Eng 2016;8:359–69. [CrossRef]
[30] Prasad, A, Sengupta, S. Nusselt number and melt time correlations for melting inside a horizontal cylinder subjected to an isothermal wall temperature condition. J Heat Transf 1988;110:340–345. [CrossRef]
[31] ANSYS, 2013, Ansys Fluent Theory Guide, Release 15.0, ANSYS Inc.

[32] Assis, E, Katsman, L, Ziskind, G, Letan, R. Numerical and experimental study of melting in a spherical shell, Int J Heat Mass Transf 2007;50:1790–804. [CrossRef]

[33] Hannoun, N, Alexiades, V, Mai, TZ. A reference solution for phase change with convection. International Journal for Numerical Methods in Fluids. 2005;48:1283–308. [CrossRef]

[34] Chunjian, P, Joshua, C, Natasha, V, Carlos, R, Sudhakar, N, Ying, Z, Chien-Hua, C, Richard B. Experimental, numerical and analytic study of unconstrained melting in a vertical cylinder with a focus on mushy region effects. Int J Heat Mass Transf 2018;124:1015–24. [CrossRef]

[35] Hirata, T, Nishida, K. An analysis of heat transfer using equivalent thermal conductivity of liquid phase during melting inside an isothermally heated horizontal cylinder. Int J Heat Mass Transf 1989;32:1663–70. [CrossRef]

[36] Jourabian, M, Farhadi, M, Sedighi, K, Darzi, AR, Vazifeshenas, Y. Melting of NEPCM within a Cylindrical Tube: Numerical study using the Lattice Boltzmann method. Num Heat Transf Part A: Applications 2012;61:929–48. [CrossRef]

[37] Park, CE, Kim, SS, Chang, KS. Branching solutions to inward melting problem in a horizontal tube. Int Commun Heat Mass Transf 1991:18:343–50. [CrossRef]

[38] Ho, C, J, Viskanta, R. Heat transfer during inward melting in a horizontal tube. Int J Heat Mass Transf 1984;27:705–16. [CrossRef]